

ICESat range and mounting bias estimation over precisely-surveyed terrain

C. F. Martin,¹ R. H. Thomas,^{1,2} W. B. Krabill,³ and S. S. Manizade¹

Received 13 June 2005; revised 18 August 2005; accepted 21 September 2005; published 25 October 2005.

[1] Prior to the launch of the Geoscience Laser Altimeter System (GLAS) on the Ice, Cloud and land Elevation Satellite (ICESat) in January 2003, topographic surveys were made by NASA's Airborne Topographic Mapper (ATM) over regions of the western United States and the Antarctic Dry Valleys to support calibration and validation of the range and pointing errors of GLAS lasers. Surveyed areas included terrain with large slopes, allowing pointing-bias estimation with as little as a few seconds of ICESat data. Range errors over sloping irregular surfaces are calculated by computing the expected GLAS return waveform and comparing it with the actual waveform. We conclude that the range bias is less than 2 cm and that pointing errors for the best available data set (Laser 2a) have rss errors less than 2 arcsec. **Citation:** Martin, C. F., R. H. Thomas, W. B. Krabill, and S. S. Manizade (2005), ICESat range and mounting bias estimation over precisely-surveyed terrain, *Geophys. Res. Lett.*, 32, L21S07, doi:10.1029/2005GL023800.

1. Introduction

[2] With the prime objective of measuring ice surface elevation changes in Greenland and Antarctica to an accuracy of a few cm/yr, the Geoscience Laser Altimeter System (GLAS) on the Ice, Cloud and land Elevation Satellite (ICESat) measures elevations of \sim 70 m diameter footprints spaced \sim 170 m apart along the satellite ground track. The range to the surface is combined with spacecraft orbital position and attitude to compute footprint geographic coordinates, i.e. where the laser beam hits the surface. For validation, we assume that both the GLAS range measurement and its pointing direction may be in error but that the orbital position has negligible error, based on state of the art orbit estimation [Schutz *et al.*, 2005]. Data time tags have been validated to a few microseconds [Magruder *et al.*, 2005] and are also a negligible error source. To validate both range and pointing throughout the satellite lifetime, GLAS measurements are required over independently-surveyed, unchanging topography for which a change in pointing produces a change in range. To obtain relatively uncorrelated errors in the estimates of range and pointing biases, we need surveyed surfaces with a variety of slopes. We first describe surveys over stable terrain areas suitable

for validation throughout the ICESat mission, then explain how these measurements are used to estimate range and pointing biases, and finally present bias estimates for GLAS laser operations to date. After the premature failure of GLAS Laser 1 after operation for only 37 days, the remaining 2 lasers have been operated intermittently, surveying along the same 33-day sub-cycle of a 91-day repeat orbit during Oct/Nov, Feb/March, and May/June. These operational periods are referenced in discussions below by laser number and a letter for the period (e.g., Laser 2a).

2. Precise Terrain Surveys

[3] As discussed below, our bias estimation technique depends upon calculating a simulated waveform to compare with the GLAS waveform received at the satellite. The distribution of elevations within a GLAS footprint, needed to simulate the return waveform, was inferred from airborne surveys using the NASA/Wallops Airborne Topographic Mapper (ATM) which has been used for over 10 years for the measurement of surface elevations on ice sheets and land with a demonstrated sub-decimeter accuracy over flight lines of hundreds of kilometers [Krabill *et al.*, 2002]. Two different areas were surveyed: the Mojave Desert in California (centered around 35°N latitude and 244°E longitude) and the Dry Valleys region in Antarctica (centered around -77.5° S latitude and 162° E longitude).

[4] Mojave Desert: Parts of California's Mojave Desert were surveyed in June, 2001, in strips 100 km long and \sim 600 m wide along 24 planned ICESat orbit tracks. Vegetation along mapped strips is sparse, consisting mostly of desert shrubs. To maximize the density of elevation points, the Mojave ATM surveys used two lasers, with an overall swath width of 400 m. Each strip was flown twice with 50% overlap between swaths. The average footprint density in the overlap region was \sim 1 per 3 m², producing \sim 1000 ATM elevations in the nominal 70-m GLAS footprint. In order to hit the surveyed strips, ICESat was pointed up to a few degrees off-nadir. During the first operational period of Laser 2 (Laser 2a), ICESat data were acquired on 8 different days pointing to 7 different ATM-surveyed strips, with off-nadir angles up to 3.3°.

[5] Dry Valleys: The Dry Valleys region in Antarctica was mapped in December 2001. This area is mostly snow free and devoid of vegetation. Due to terrain constraints, the valley floors and edges were mapped with overlapping ATM swaths in directions approximately perpendicular to planned ICESat ground tracks, thus eliminating the need for ICESat off-nadir pointing except for passes near the ends of the valleys. The high Antarctic latitudes provide a higher spatial density of ICESat orbit tracks than the Mojave area.

¹EG&G Technical Services, NASA Wallops Flight Facility, Wallops Island, Virginia, USA.

²Also at Centro de Estudios Científicos (CECS), Valdivia, Chile.

³Hydrospheric and Biospheric Sciences Laboratory, Cryospheric Sciences Branch, NASA Goddard Space Flight Center, Wallops Island, Virginia, USA.

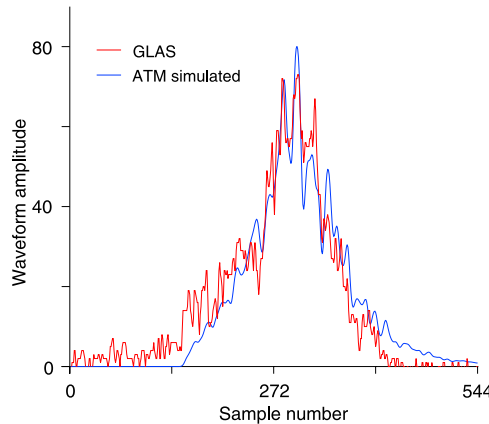


Figure 1. GLAS waveform, taken on 11 October 2003 at $10^{\text{h}}33^{\text{m}}13.523^{\text{s}}$ UTC, and ATM simulated waveform for Antarctic Dry Valley footprint centered at -77.3253° S latitude and 160.922° E longitude. Maximum correlation between waveforms is obtained by shifting simulated waveform 2.6 nsec (samples) to the left, corresponding to a range residual of -0.39 m.

For Laser 2a, usable validation data were acquired for 15 different ICESat passes.

3. Estimation Technique

[6] GLAS range measurements are computed from the time delay between pulse transmission and return, with corrections for atmospheric delays, solid Earth tides, and other effects. Over ice sheets and land, the return pulse is recorded in a range window of 544 1 ns bins. In “standard” ICESat processing, the position of the reflecting surface in the range window is based on a Gaussian fit to the return pulse. However, an irregular surface only means that the simulated waveform based on ATM surveys will be more complex than a simple Gaussian and there may be more uncertainty in comparison with the GLAS waveform. For the most accurate waveform computation, one also needs the reflectivity characteristics of the surface; however, these are not readily available and we assume here a constant reflectivity over the footprint.

[7] The simulated GLAS return-pulse waveform is calculated using: (a) the GLAS transmitted pulse width (~ 11 nsec at the $1/e^2$ point), (b) the measured transmitted pulse shape (variable from one laser to the next but more or less Gaussian), (c) the 3-d elevation distribution within the laser footprint out to a radius at which the beam amplitude drops to $<0.5\%$ of peak amplitude, and (d) the sensitivity of the GLAS telescope to returns within its field of view. This procedure is similar to that of *Harding and Carabajal* [2005], although the emphasis here is on matching pulse arrival times rather than waveform shapes since our surfaces contain little vegetation and displacements of surface position may make little change in the simulated waveform shape. The center of the ATM surface used for waveform simulation is always based on the current estimate (i.e., latest iteration) of GLAS pointing and could be twenty or more arcsecs away from the footprint location given on the GLA14 data file used. Figure 1 shows a sample of observed

and simulated waveforms for a Dry Valley pass from a spot for which surface slope was $>22^{\circ}$.

[8] To estimate pointing errors from differences between calculated and measured ranges, we need to calculate the sensitivity of ranges to changes in pointing. The GLAS laser is mounted on the spacecraft Optical Bench (OB) as described by *Schutz et al.* [2005] and the laser is pointed very close to the OB negative z axis as shown in Figure 2. Mathematically, the laser is mounted on axes rotated by an angle X about the OB x axis and by an angle Y about the OB y axis. In OB coordinates, the laser pointing direction thus has the components $[\sin Y \cos X, -\sin X, -\cos Y \cos X]$. Our objective is to relate laser range errors to errors in the X and Y rotation angles. ATM positions are in earth-fixed coordinates, so the pointing direction and the satellite position were converted to ITRF (International Terrestrial Reference Frame) coordinates. Pointing directions were first transformed from OB to ICRF (International Celestial Reference Frame) coordinates using “obatt” files obtained from the University of Texas CSR web site (ftp.csr.utexas.edu/pub/icesat/pad) and then to ITRF coordinates using standard ICESat “ANC04” ancillary data files. The components of the vector p in Figure 2 can then be expressed as

$$\begin{bmatrix} p_1 \\ p_2 \\ p_3 \end{bmatrix} = \mathbf{T}_{\text{ITRF}/\text{ICRF}} \mathbf{T}_{\text{ICRF}/\text{OB}} \begin{bmatrix} \sin Y \cos X \\ -\sin X \\ -\cos Y \cos X \end{bmatrix} \quad (1)$$

where the transformation matrices go between the frames indicated by the subscripts.

[9] To a first approximation, the ATM surveyed strips may be considered planar over the area of a GLAS footprint. To calculate the sensitivity of the GLAS range to pointing angle errors, we fit the ATM surface within the footprint to a plane and then calculate the range from the satellite to the plane. Any point in the planar surface can be expressed as

$$z_{\text{ATM}}^i = ax_{\text{ATM}}^i + by_{\text{ATM}}^i + c + e^i \quad (2)$$

where a, b, and c are constants and e^i is the fit error of the i'th point. The constants are estimated for each footprint by

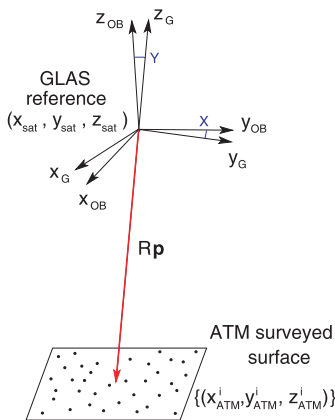


Figure 2. Geometry of ICESat axes and their relation to ATM surfaces. The $(x_{\text{OB}}, y_{\text{OB}}, z_{\text{OB}})$ are Optical Bench axes and the (x_G, y_G, z_G) are GLAS laser axes. X and Y are the rotation angles between these coordinates.

Table 1. Estimated Range Biases Using ICESat Passes Over Mojave

Laser Operating Period	Data Release	Number of Passes	Number of Obs.	RMS, cm	Bias, cm	Sigma, cm
1	18	3	1349	26.7	1.78	1.5
2a	21	8	3035	24.5	-0.67	1.0
2b	16	6	1841	28.9	2.07	1.7
2c	17	5	3152	27.9	0.12	1.2
3a	22	3	1783	19.6	-2.01	1.0
3b	19	6	1551	23.7	3.66	1.6

a least squares estimation which minimizes the sum of squares of the e^i 's. We assume that the transformation matrix $T_{\text{ITRF/ICRF}}$ has been applied to the satellite coordinates and that the coordinates in Figure 2 are ITRF coordinates. We can then express the vector from the satellite to the plane as

$$R \begin{bmatrix} p_1 \\ p_2 \\ p_3 \end{bmatrix} = \begin{bmatrix} x_{\text{ATM}} \\ y_{\text{ATM}} \\ ax_{\text{ATM}} + by_{\text{ATM}} + c \end{bmatrix} - \begin{bmatrix} x_{\text{sat}} \\ y_{\text{sat}} \\ z_{\text{sat}} \end{bmatrix} \quad (3)$$

This equation can be solved for R to give

$$R = (ax_{\text{sat}} + by_{\text{sat}} + c)/(p_3 - ap_1 - bp_2) \quad (4)$$

Since the components of the vector p are functions of the mounting angles via equation (1), one can easily obtain the partial derivatives of R with respect to X and Y. For each GLAS measurement during an ICESat pass over a surveyed area (typically 10–20 seconds long), we then have the range error (or residual)

$$\delta R_i = b_r + \frac{\partial R_i}{\partial X} \delta X + \frac{\partial R_i}{\partial Y} \delta Y + \varepsilon_i, \quad i = 1, N \quad (5)$$

where δR_i is the range residual which would be calculated from differences between GLAS and simulated waveforms such as are shown in Figure 1, b_r is a range bias, δX and δY are mounting biases (on the spacecraft, but on the surface they become pointing biases and we use the terms somewhat interchangeably), and ε_i is measurement noise (as well as perhaps other errors which could not be modeled). We estimate the parameters b_r , δX , and δY using least squares to minimize the sum of the $(\varepsilon_i)^2$ for the N measurements of the ICESat pass. Iteration is required because the estimation is non-linear and the assumption of a planar surface for partial derivative computation is only approximate. Dry Valley passes typically have a few tens of ICESat observations while Mojave passes have a few hundred. Nevertheless, because of large surface slopes, pointing biases are generally well determined for each pass at both sites. Results show that, although pointing errors vary from pass to pass, the range bias appears to be stable to better than a decimeter during an ICESat operations period. Thus, we have calculated range bias for each of these periods. For example, for Laser 2a, we solved for a single range bias, but we calculated δX and δY for each pass within Laser 2a. To allow for the possibility that ICESat pointing could have regionally-dependent errors, we also obtained

independent solutions for the Mojave and Dry Valleys regions.

4. Results: Range Bias

[10] The Mojave and Dry Valley sites were chosen primarily for their large surface slopes, which make GLAS ranges particularly sensitive to pointing errors. For example, a 1 arcsec pointing error to a 2° slope produces a 10 cm error in derived elevations, rising to more than a meter per arcsec for a 20° slope. For measurements to the 22° surface with waveforms shown in Figure 1, the sensitivity is 15 cm per arcsec of X angle error and 1.18 m per arcsec of Y angle error. For large slopes there will be large residuals and high residual noise levels, so it is not surprising that there is considerable scatter in the estimates of range bias from individual passes, especially for the short Dry Valley passes. Nevertheless, range bias estimated from a single pass seldom exceeds 20 cm for the Dry Valleys and 10 cm for Mojave passes.

[11] Since all our range-bias estimates were small throughout the ICESat mission, with no evidence for significant temporal variation, estimation accuracies can be substantially enhanced by combining passes. We thus estimated a range bias for each operations period, with pointing biases assumed independent from one pass to another. It should be emphasized that the estimation of pointing errors for each ICESat pass basically eliminates the effects of ICESat pointing errors on the range bias estimates. The only residual effects should be due to Instrument Star Tracker (IST) instrumental errors [Schutz et al., 2005], and these effects are considered minor. Range biases estimated at the two sites are summarized in Tables 1 and 2. ICESat data used were limited to those with residuals less than 1 meter, and correlation coefficients between GLAS and calculated waveforms of 0.95 or greater. The sigmas shown are the formal estimation sigmas scaled by the rms and then multiplied by a factor of 2. The rms includes true measurement noise, ATM elevation errors (having short spatial wavelengths), and other modeling errors. For ice-sheet mapping, ATM elevation uncertainty has been estimated to be around 8 cm [Krabill et al., 2002] over small areas using a single GPS reference station for trajectory estimation. These errors are primarily due to tropospheric modeling uncertainties and vary between aircraft flights. Mojave ATM mapping took 4 days with 4 or more ground reference stations each day. Dry Valley mapping used only one GPS reference station but was performed over an 8 day period and with much shorter baselines. The scaling of the rms by the additional factor of 2 attempts to account for residual systematic ATM errors in each of the Mojave and Dry Valley survey flights.

Table 2. Estimated Range Biases Using ICESat Passes Over Dry Valleys

Laser Period	Release Number	Number of Passes	Number of Obs.	RMS, cm	Bias, cm	Sigma, cm
1	18	9	141	24.3	6.65	6.5
2a	21	15	430	29.1	-0.33	3.3
2b	16	5	121	16.8	3.75	3.8
2c	17	4	70	23.5	4.84	6.5
3a	22	13	514	30.8	-3.77	3.4
3b	19	9	206	23.3	1.59	3.6
All		55	1482	27.6	-0.14	1.8

[12] Also shown in the tables are combined biases for each area, assuming a common range bias for all operation periods. The overall estimate is 0.34 ± 0.5 cm for Mojave and -0.14 ± 1.8 cm for the Dry Valleys. Thus, while a systematic change in range bias from one laser or operations period to another cannot be ruled out, it is clear that both the variation and the overall bias are at most a few centimeters. These results are also consistent with an estimated bias of <2 cm for Laser 2a by Fricker *et al.* [2005] based on an ICESat pass over the salar de Uyuni in Bolivia.

5. Results: Pointing Biases

[13] All passes over ATM-surveyed strips are relatively short – a few seconds for the Dry Valleys and a few tens of seconds for the Mojave. Accordingly, estimated pointing biases are significantly affected by IST instrumental errors, with the exception of Laser 2a and Laser 3b. Only Laser 2a has been corrected for temporal variations during a revolution due to thermal distortions of the telescope orientation as the spacecraft moves in and out of sunlight (M. Sirota et al., The transmitter pointing determination on the Geoscience Laser System, *Geophysical Research Letters*, 2005). Pointing biases estimated for Laser 2a are shown in Figure 3 as a function of day number for both the X and Y mounting angles. The mean for the X angle bias is 0.03 arcsec with an rss of 1.36 arcsec. A linear fit to the data shows an overall trend of only 1–2 arcsec over the total data span. For the Y angle, the mean bias is -0.26 arcsec with an rss of 1.39 arcsec and an even smaller trend. It should be noted that the Laser 2a operations period included several temperature changes intended to reduce telescope shadowing, and these changes also induced changes in pointing bias. Given these problems, the results are remarkably good and very close to the pre-mission plan of 1.5 arcsec.

[14] In Figure 4, the Laser 2a mounting bias estimates are plotted as a function of sun angle (angle in orbit plane of satellite minus sun direction mapped into orbit plane plus 90°). For the X angle the estimated errors show little overall dependence on sun angle, but the trends in the two Mojave periods suggest some small systematic errors in modeling of either temporal changes or variations with sun angle. For the Y angle, the Dry Valley estimates show mainly random scatter. On the other hand, the estimates from Mojave, in addition to showing a mean difference around 1 arcsec, again show some evidence of linear trends for regions around 0° and 270° . However, the overall level of the errors

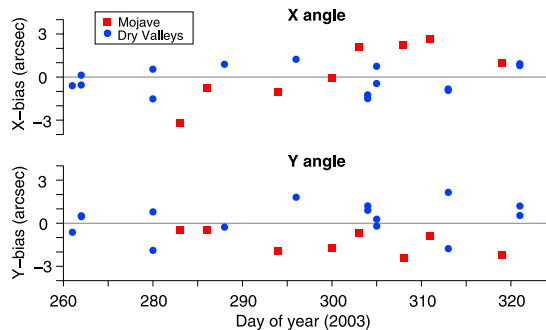


Figure 3. Estimated GLAS pointing biases for Laser 2a from Mojave and Dry Valley passes as functions of time. Mean values are $0.03''$ for X and $-0.26''$ for Y.

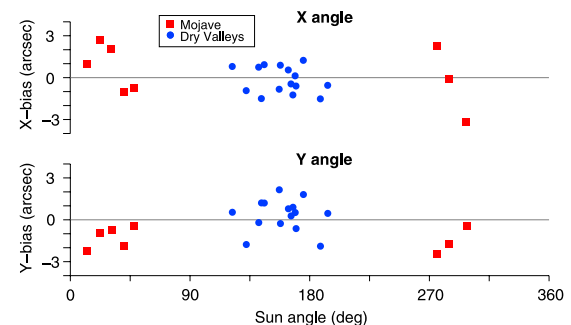


Figure 4. Estimated GLAS pointing biases for Laser 2a plotted as functions of sun angle.

is quite small and the apparent systematic behavior may be only a statistical anomaly in view of the relatively small number of points.

6. Summary

[15] Validation of ICESat data over ATM-surveyed areas gives an estimated overall range bias of 0 ± 2 cm, with little indication of variations from one laser to another, or from one operations period to another. Considering that Mojave and the Dry Valleys are widely separated geographic areas, and with the Fricker result from Bolivia providing a third area, there is also no indication of geographic range bias dependence. Pointing-bias calibrations for the operational period with (nearly) complete refinement of laser pointing (Laser 2a) show rss errors less than 2 arcsec, again with the agreement between Mojave and the Dry Valleys indicating little geographic dependence of errors. Additional comparisons using ICESat data from all operations periods will refine assessments of measurement performance and improve measurements of elevation change.

[16] **Acknowledgments.** We thank NASA's ICESat SCF for distribution of the ICESat GLA12 and GLA14 data files and ANC04 ancillary files, and for responding promptly to various special data requests. This research was supported through NASA Contract NAS5-99003 to ICESat Team Member R Thomas. We gratefully acknowledge the yeoman's service of Bob Schutz in twice reviewing this paper.

References

- Fricker, H. A., A. Borsa, B. Minster, C. Carabajal, K. Quinn, and B. Bills (2005), Assessment of ICESat performance at the salar de Uyuni, Bolivia, *Geophys. Res. Lett.*, 32, L21S06, doi:10.1029/2005GL023423.
- Harding, D. J., and C. C. Carabajal (2005), ICESat waveform measurements of within-footprint topographic relief and vegetation vertical structure, *Geophys. Res. Lett.*, 32, L21S10, doi:10.1029/2005GL023471.
- Krabill, W., W. Abdalati, E. Frederick, S. Manizade, C. Martin, J. Sonntag, R. Swift, R. Thomas, and J. Yungel (2002), Aircraft laser altimetry measurement of elevation changes of the Greenland ice sheet: Technique and accuracy assessment, *J. Geodyn.*, 34, 357–376.
- Magruder, L., E. Silverberg, C. Webb, and B. Schutz (2005), In situ timing and pointing verification of the ICESat altimeter using a ground-based system, *Geophys. Res. Lett.*, doi:10.1029/2005GL023504, in press.
- Schutz, B. E., H. J. Zwally, C. A. Shuman, D. Hancock, and J. P. DiMarzio (2005), Overview of the ICESat Mission, *Geophys. Res. Lett.*, doi:10.1029/2005GL024009, in press.

W. B. Krabill, Hydrospheric and Biospheric Sciences Laboratory, Cryospheric Sciences Branch, NASA Goddard Space Flight Center, Code 6114, Wallops Island, VA 23337, USA.

C. Martin, S. S. Manizade, and R. H. Thomas, Centro de Estudios Científicos (CECS), Avenida Arturo Prat 514, Casilla 1469, Valdivia, Chile. (chreston_2@comcast.net)